Revealing the Orientation of Nystatin and Amphotericin B in Lipidic Multilayers by UV−Vis Linear Dichroism

S. Lopes[†,‡] and M. A. R. B. Castanho*[,†,‡]

Centro de Química-Física Molecular, Instituto Superior Técnico, Av. Rovisco Pais, 1049-001 Lisboa, Portugal, and Departamento de Química e Bioquímica da Faculdade de Ciências da Universidade de Lisboa, Campo Grande, Ed. C8, 1749−016 Lisboa, Portugal

Received: January 17, 2002; In Final Form: April 22, 2002

Amphotericin B UV−Vis absorption linear dichroism data was combined with Nystatin steady-state fluorescence linear dichroism data to calculate their orientational probability density functions in multilayers of dipalmitoylphosphatidylcholine (DPPC), DPPC+cholesterol and arachidic acid+cholesterol multilayers. The cholesterol effect is striking on both the mean orientation and range of allowed orientations. The mean becomes closer to the layers normal (from 8.6° to 2.3°) in DPPC multilayers when cholesterol is present and the range (i.e., full distribution width) narrows from ≅40° to ≅10°. However, a small fraction of the antibiotic eventually remains parallel to the multilayer surface, possibly adsorbed to it. The results favor the pore model for the biochemical mode of action of the antibiotics. Moreover, a direct involvement of the sterols is suggested.

Introduction

Polyene antibiotics, such as Nystatin (Nys) and Amphotericin B (AmB), Figure 1, have long been used as therapeutic agents against systemic fungal infections.[1] Opportunistic infections as a consequence of weakened immunity defenses, such as from AIDS or from many cancer therapies,[2,3] renewed the scientific interest in this class of molecules. Although it is well-established that these antibiotics act at the membrane level[1] and that the sterols play a role in their biochemical action (increased permeability of the membranes with loss of low molecular weight metabolites), the molecular details of the structure and organization of the antibiotics inside the phospholipidic membranes are still far from understood. The formation of transmembrane channels composed of alternate sterol and polyene molecules was proposed,[4] but direct evidence of such organization is rather scarce. The model largely relies on chemical intuition. Another polyene antibiotic, Filipin (Figure 1), having a similar chemical nature, is thought to form large aggregates in the core of the phospholipidic bilayers.[4] Moreover, the formation of a stable complex between vertically oriented dipalmitoyl phosphatidic acid and horizontally oriented AmB molecules was recently demonstrated in monolayers.[5] Our main goals are to determine the orientational distribution function of Nys and AmB (such distribution is assumed to be the same allowing data from both molecules to be combined, see below) in the presence and in the absence of a sterol and to conclude on their relevance to the biochemical action of the antibiotics. Published papers on this subject are rare and mainly devoted to monolayers.[5−14]

Materials and Methods

Arachidic acid (Analar, Germany), AA, and all other chemicals (Sigma, St. Louis, MO) were 99% pure (except for AmB, 80% pure). Solvents were from Merck (spectroscopic grade).

* Corresponding author. Address: Departamento de Química e Bioquímica da Faculdade de Ciências da Universidade de Lisboa, Campo Grande, Ed. C8 − 6° Piso, 1749-016 Lisboa, Portugal. Telephone: 351 21 7500931. Fax: 351 21 7500088. E-mail: pcmcastanho@popsrv.ist.utl.pt.

† Instituto Superior Técnico.

‡ Faculdade de Ciências da Universidade de Lisboa.

Langmuir Blodgett (LB) films were prepared with a NIMA (Coventry, U.K.) trough. A 20 μL sample of AA solutions in chlorophorm (1 mM) with or without polyene antibiotic (from 1 mM stock solution) was placed in the surface of the subphase, 1 mM $Pb(NO_3)_2$, and let to evaporate for 1 h. The molar AA/cholesterol/antibiotic ratios were 4:1:1. Depositions were carried out over 1 mm thick quartz plates specially prepared by Precision Glass & Optics (Santa Ana, CA) at a surface pressure of 40 mN/m. AA samples had 13 layers on each side of the quartz plate.

Samples of aligned dipalmitoylphosphatidylcholine (DPPC) multilayers were obtained by evaporation of the solvent. First, multilamellar vesicles were prepared. The lipid solution in chloroform was dried in a round flask under a N_2 flow and placed in a vacuum overnight. Then the lipid solutions were resuspended in Millipore water by cycles of vortexing/heating. A drop of the suspension (25 μL) with or without sterol and/or antibiotic was spread on one surface of a quartz plate and the solvent was slowly evaporated under a controlled N_2 flow with a pipet in order to make the film as uniform as possible. The final molar ratios of lipid to sterol (if present) were 2:1, and the antibiotic content was always 3.3% molar. Mixed spreading of lipid and antibiotic leads to a miscible system.[5]

UV−Vis absorption measurements were carried out in a Shimadzu spectrophotometer (model UV-3101 PC). Dichroic ratios were determined using Glan-Thompson polarizers in homemade stands. Blank correction was carried out by reading both sample and blank (DPPC or AA+cholesterol films) against air, and subtracting afterward. However, in DPPC/cholesterol/AmB samples a more sophisticated process was needed due to turbidity. Turbidity background was accounted for using a methodology similar to the one described in ref 15. However, equations relating absorption and turbity were replaced by equations that took into account the inhomogeneous distribution of the chromophores and heavy contribution from light scattering.[16] Namely, a two-step procedure was followed. (1) First, the nonabsorbing red vicinity of the absorption spectrum was fitted with eq 1 to calculate the value of the constants k_1 and k_2

10.1021/jp020160s CCC: $22.00
Published on Web 06/22/2002

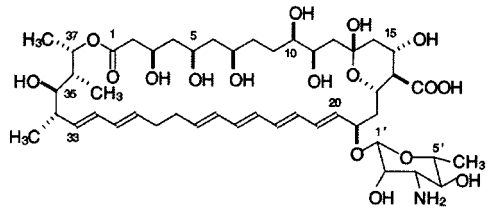

Nystatin A_1

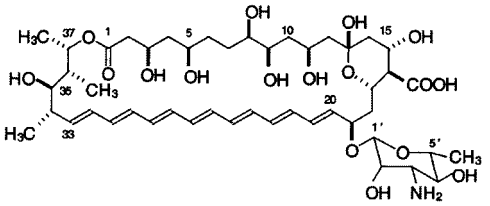

Amphotericin B

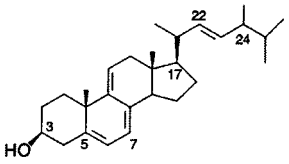

DHE

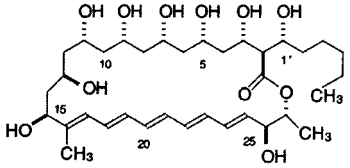

Filipin III

Figure 1. Chemical structure of the most abundant and representative molecules of the Nystatin, Amphotericin, and Filipin families. DHE is also represented.

$$T(\lambda) = \frac{\kappa_1}{\lambda^4}\left(1 - \frac{\kappa_2}{\lambda^2}\right) \tag{1}$$

where $T(\lambda)$ is the turbidity signal. (2) Second, the absorption spectrum, $A(\lambda)$, was obtained:

$$A(\lambda) = \frac{S(\lambda)\lambda^2}{\lambda^2 - \kappa_2} - \kappa_1\lambda^{-4} \tag{2}$$

where $S(\lambda)$ is the recorded spectrum. In practice, the turbidity background signal is almost linear with λ, and empirical linear baseline correction obtained bysetting both red and blue extremes to zero yields similar results.

The quartz plates were mounted in a goniometer (Optosigma, SL) which replaced the usual sample holder. A spectrofluorimeter SLM-Aminco 8100 was also used, equipped with a 450 W Xe lamp and double monochromators in both excitation and emission, as well as a quantum counter. Dichroic ratios and fluorescence intensity ratios were measured in the range of 0−72° and 18−72°, respectively. Nystatin excitation and emission wavelengths were, respectively, 324 and 418 nm.

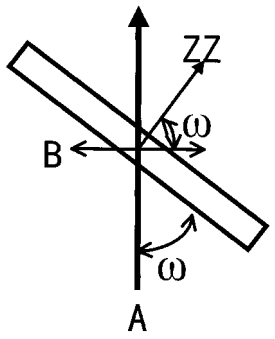

Figure 2. Experimental setup for $\langle P_2\rangle$ calculation with UV−Vis absorption measurements. The *ZZ* axis is the system director, A is the incident beam, and B is the polarization direction.

Dichroic ratios were measured at 344 nm for dehydroergosterol, DHE, and 417 nm for AmB but were largely independent of the wavelength in the lowest energy absorption band experimentally accessible ($S_2 \leftarrow S_0$).

All experiments were carried out at room temperature.

Theorectical Background and Data Analysis

Data analysis methodologies are generally described in refs 17 and 18. Since only $\langle P_2\rangle$ and $\langle P_4\rangle$ are experimentally accessible, a combination of the maximum entropy method with the formalism of the Lagrange multipliers method is used to describe the single particle distribution function, $f(\psi)$, where ψ is the angle between the long axis of a cylindrically symmetric molecule and the director of the system (normal to the multilayers plane). In practice, one seeks the values of the constants λ_2 and λ_4 (Langrange multipliers) that satisfy eqs 3−5:

$$\langle P_2\rangle = \int_0^\pi \sin\psi P_2(\cos\psi) f(\psi)\, d\psi \tag{3}$$

$$\langle P_4\rangle = \int_0^\pi \sin\psi P_4(\cos\psi) f(\psi)\, d\psi \tag{4}$$

$$f(\psi) = \frac{\exp(\lambda_2 P_2(\cos\psi) + \lambda_4 P_4(\cos\psi))}{\int_0^\pi \sin\psi\, \exp(\lambda_2 P_2(\cos\psi) + \lambda_4 P_4(\cos\psi))\, d\psi} \tag{5}$$

where P_L is the Legendre polynomial of Lth order and $\langle P_L\rangle$ is the ensemble average of $P_L(\cos\psi)$, the Lth rank order parameter.

The term $f(\psi)$ calculated this way represents the broadest possible angular distribution that is compatible with the experimentally determined values of $\langle P_2\rangle$ and $\langle P_4\rangle$. Here, $f(\psi)\sin(\psi)$ is the population density probability function, i.e., the probability of finding a transition moment between ψ and $\psi+d\psi$ is $f(\psi)\sin(\psi)\, d\psi$. The constants λ_2 and λ_4 were determined by a least-squares method where the λ_2, λ_4 space was searched for the best solution of eqs 3 and 4. The (λ_2, λ_4) solutions lead the two members in eqs 3 and 4 to be identical with a maximum error of 4.8×10^{-4}% relative to $\langle P_2\rangle$ and $\langle P_4\rangle$ simultaneously, in all the studied systems, except DPPC+cholesterol (0.02%).

$\langle P_2\rangle$ was calculated using the setup depicted in Figure 2 and eq 6. Inclusion of the $\sin\omega$ term accounts for the increasing area of illuminated sample as ω decreases. $\langle P_4\rangle$ was calculated as proposed by Kooyman et al.,[18] i.e., by means of steady-state fluorescence spectroscopy (eq 7) having excitation and emission in a 90° angle geometry (Figure 3). The strong collision model framework[18] was adopted. A single correlation time, τ_0, is present which can be interpreted as the time during which the transition moment has a particular, fixed orientation relative to the director (eq 11) and τ is the intrinsic fluorescence lifetime

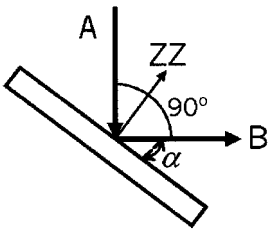

Figure 3. Experimental setup for $\langle P_4 \rangle$ calculation with steady-state fluorescence measurements. The *ZZ* axis is the system director and A and B are the directions of excitation and detection, respectively.

of the fluorophore. Assuming that $\langle P_2 \rangle$ and w are the same in macroscopically ordered (e.g., LB films) and disordered (e.g., vesicles) samples, eq 12 holds, where r is the steady-state fluorescence anisotropy. The values of r for Nystatin are available in the literature for lipid bilayers.[19] The value for AA multilayers was assumed to be identical. This is a reasonable aproximation because r does not severely depend on the host matrix acyl chain[20]

$$\frac{\sin(\omega)A_\omega}{A_{\omega=(\pi/2)}} = 1 + \frac{3\langle P_2 \rangle}{(1 - \langle P_2 \rangle)n^2}\cos^2\omega \tag{6}$$

where A_ω is the absorbance at angle ω and n is the relative refraction index; $n = 1.5$.[18]

$$\frac{I_{vh}}{I_{vv}} = a \sin^2\alpha + b \tag{7}$$

Here, I_{vh} and I_{vv} are the fluorescence emission intensities measured having excitation and emission polarizers set to "vertical" and "horizontal" positions in the laboratory frame, or both "vertical", respectively.

$$a = \frac{\left[\left(\frac{3}{7}\langle P_4 \rangle + \frac{4}{7}\langle P_2 \rangle - \langle P_2 \rangle^2\right)w + \langle P_2 \rangle^2 - \langle P_2 \rangle\right]}{c} \tag{8}$$

$$b = \frac{1}{3}\frac{\left[1 - \left(\frac{2}{5} + \frac{36}{35}\langle P_4 \rangle + \frac{4}{7}\langle P_2 \rangle - 2\langle P_2 \rangle^2\right)w - 2\langle P_2 \rangle^2 + \langle P_2 \rangle\right]}{c} \tag{9}$$

$$c = \frac{1}{3}\left[1 + \left(\frac{4}{5} - \frac{4}{7}\langle P_2 \rangle + \frac{27}{35}\langle P_4 \rangle - \langle P_2 \rangle^2\right)w + \langle P_2 \rangle^2 - 2\langle P_2 \rangle\right] \tag{10}$$

$$w = \frac{\tau_0}{\tau_0 + \tau} \tag{11}$$

$$r = \frac{2}{5}[\langle P_2 \rangle^2 + w(1 - \langle P_2 \rangle^2)] \tag{12}$$

Assuming that Nys and AmB share the same biochemical mode of action (both molecules are remarkably similar (see Figure 1 and ref 21) and share many common functional properties[19,22]) and taking advantage of the high absorptivity of AmB and the high fluorescence quantum yield of Nys in lipidic environment, the data obtained from both molecules was combined to obtain a single pair of $\langle P_2 \rangle$ and $\langle P_4 \rangle$ values. $\langle P_2 \rangle$ was obtained from the absorption data of AmB (equation 6) and $\langle P_4 \rangle$ was obtained from fluorescence emission data of Nys (eq 7). $\langle P_2 \rangle$ of DHE was also calculated by means of eq 6.

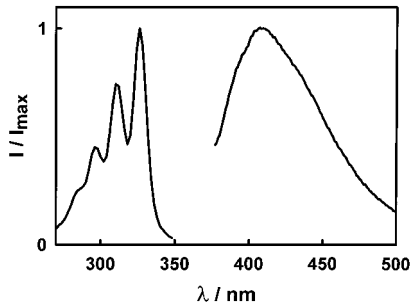

Figure 4. Normalized excitation and emission spectra of Nys in AA+cholesterol multilayers at room temperature ($\lambda_{exc} = 324$ nm; $\lambda_{em} = 418$ nm).

TABLE 1: Second and Fourth Rank Order Parameters for Each of the Studied Systems[a]

molecule	multilayer medium	$\langle P_2 \rangle$	$\langle P_4 \rangle$	λ_2	λ_4
Nys/AmB	DPPC	0.760	0.677	1.308025	3.843583
	DPPC+Chol	0.850	0.938[b]	−19.56667	54.96667
	AA+Chol	0.744	0.784	−0.40575	7.569334
DHE	DPPC	0.879			

[a] λ_2 and λ_4 are Lagrange multipliers that result from the application of the maximum entropy method to obtain the orientational distribution functions. [b] The average $\langle P_4 \rangle$ value obtained was actually slightly more than 0.938. However, this value is inside the error margin and is the majorant of physically admissible values regarding $\langle P_2 \rangle = 0.850$.[18]

The correction factors were dealt with in detail by Kooyman et al.[18] Two significant factors should be taken into account: (1) the angular dependent propagation of light passing through an interface of two isotropic media having different refraction indices, and (2) the transmission fraction of light passing through a boundary of two media being dependent on its polarization state. Snell's law corrects the first factor while the second is corrected by means of Fresnel's law; corrections were made accordingly. I_{vh}/I_{vv} (eq 7) was corrected by the geometry factor G ($G = I_{hv}/I_{hh}$) to account for different transmitances of the emission monochromator for vertically and horizontally polarized light. G, an instrumental factor, was determined in homogeneous solution for better accuracy.

Results and Discussion

The vibronic progression of both the absorption and emission spectra of the antibiotics in aligned samples (e.g., Figure 4) is typical from monomeric polyenes[23] as expected. Exciton interaction is typical of greater antibiotic/lipid ratios.[24]

Experimentally calculated $\langle P_2 \rangle$ and $\langle P_4 \rangle$ values are presented in Table 1. Constants λ_2 and λ_4 were calculated so that orientational distribution functions could be obtained (eq 5). Such distributions are depicted in Figure 5. Although information on the structural organization of lipidic multi-bilayers formed by evaporation of the solvent, as described in Materials and Methods, is abundant and sound,[25] the alignment of the system was further checked comparing $\langle P_2 \rangle$ and $\langle P_4 \rangle$ of *trans*-parinaric acid, a tetraene fatty acid to the ones obtained in LB films of DPPC.[18] The results were identical; therefore, DPPC multilayers are aligned. Moreover, introduction of a sterol did not influence the system drastically since DHE, a sterol related to ergosterol (Figure 1), presents a $\langle P_2 \rangle$ value close to 1 (Table 1). This result would not be possible to obtain if the system was not aligned. Unfortunately, more detailed information on the orientation of this sterol is prevented by the fact that the angle between molecular axis and transition moment is unknown (to our best knowledge) in cis-trans polyenes such as DHE. For

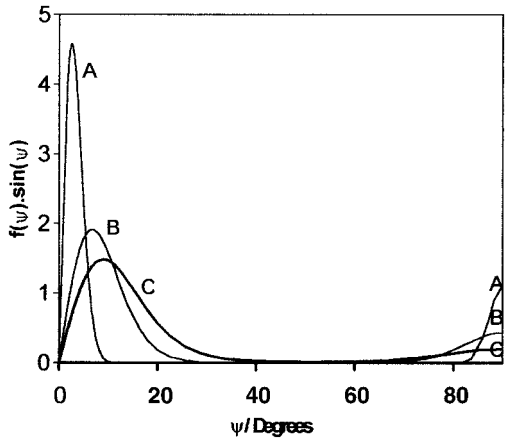

Figure 5. Probability density functions for Nys in DPPC-cholesterol (A), AA-cholesterol (B), and DPPC (C) multilayers at room temperature.

all-trans polyenes, such as Nys and AmB, this angle is rather small,[26−28] enabling meaningful conclusions to be drawn from $\langle P_2 \rangle$ and $\langle P_4 \rangle$ directly.

At a first glance it would seem possible that the orientational distributions of the antibiotics presented in Figure 5 were biased due to the presence of polyene antibiotic in the water layers that alternate with the lipidic bilayers in supported multilayers. However, it should be noticed that water and lipidic layers have similar volumes[25] and the partition coefficient largely favors the lipidic phase ($K_p = 1.4 \times 10^3$ for Nystatin in gel phase DPPC small unilamellar vesicles[19]). Therefore, the fraction of antibiotic molecules present between lipid bilayers is very small: ≅1400 times fewer molecules than the ones interacting with the lipids. Moreover, for Nystatin, the fluorescence quantum yield of the molecules in aqueous medium is very low (<0.003[23]), so the fluorescence signal from the aqueous layers is nonsignificant.

Figure 5 shows that the polyene antibiotics in the absence of cholesterol have an orientational distribution that is fairly broad (full width ≅ 40°) and peaks at 8.6°, almost collinear to the bilayer's normal. In the presence of cholesterol, the antibiotics lie practically perpendicular to the planes of the bilayer and highly ordered (the range of allowed orientations is restricted to ≅10°). In LB films of AA and cholesterol, the distribution is neither as narrow nor so close to the director axis. Ockman previously noticed in a qualitative way a pronounced effect of cholesterol in the alignment of the antibiotics in monolayers.[6,7] Figure 5 shows that the sterol contributes not only to a reorientation of the antibiotic but also to its order degree. This result is a clue that points to a role of the sterol in the antibiotic's mode of action, in agreement with experiments carried out in vivo in fungus cells.[29] The high order of the antibiotics orientation appearing upon cholesterol addition is compatible with the biochemical mode of action model that considers the formation of pore-like structures composed of a packing of alternate sterols and antibiotics in a very organized array.[4] Some authors[30−33] proposed that the sterol role is not to participate in the pore formation itself but to "pack" the phospholipids in fluid membranes in a more favorable arrangement (i.e., more dense) for antibiotic association. This idea is supported by permeability studies that show that the antibiotic action is not dependent on the presence of sterol in the gel-phase membranes. At variance, structural data presented in Figure 5 show that cholesterol is capable of influencing the antibiotic organization even in gel-phase DPPC. The functional properties of the pore may not be significantly different, but our data point toward a direct sterol/antibiotic interaction. An alternative model[34] that considers sterol exclusion of the membrane due to antibiotic action is not compatible with our results.

Although being a small contribution to the overall distribution, the small peaks at 90° (present in both systems) deserve some attention. Several reasons can be pointed out: (1) a fraction of the fluorophores lies parallel to the bilayer plane, (2) a fraction of the bilayer has macroscopic defects and involves antibiotic molecules, (3) the peaks are spurious and result from the data analysis method. In practice, it is hard to distinguish between hypotheses 2 and 3 because $f(\psi)\sin(\psi)$ can only lead to bimodal distributions if one of the peaks is at 90°, i.e., a disordered subpopulation of antibiotics would lead to a biased distribution having a peak at 90°. To better ascertain the causes of such a peak, measurements were also carried out in LB multilayer films composed of arachidic acid and cholesterol. Arachidic acid multilayer deposited films are known to be well ordered and organized,[35] therefore the contribution of disordered regions in the sample should be very small compared to films prepared by evaporation. The presence of a bimodal distribution in this system points toward the exclusion of hypothesis 2. Although an option for hypothesis 1 or 3 cannot be firmly taken from the data, several researchers proposed that AmB could adsorb to the bilayer surface, rendering the transition moment perpendicular to the system director axis.[6,8,11,20] If this is the case, then it can be concluded that the fraction of antibiotic molecules adsorbed to the bilayers is very small.

Conclusions

Our results are consistent with three conclusions. (1) AmB and Nys alone insert in the membrane with an average orientation that is close to the phospholipid bilayer plane normal (≅ 8.6°). (2) Cholesterol modulates the antibiotic orientation in the DPPC membranes, making them narrower (full width from ≅40° to ≅10°) and reducing the angle relative to the bilayer normal (becomes ≅ 2.3°). (3) The existence of a fraction of antibiotic molecules adsorbed parallel to the membranes surface is compatible with our results.

The conclusions reached in this work concur with some that can be found in the literature,[6,7] but the quantitative reasoning over the orientational distributions brings new insights into the biochemical mode of action of AmB and Nys.

Acknowledgment. The authors acknowledge Fundação para a Ciência e Tecnologia (Portugal) for funding and thank Dr. A. Coutinho (Faculty of Sciences, University of Lisbon and Instituto Superior Tecnico, Lisboa, Portugal) and Dr. M. Prieto (Instituto Superior Tecnico, Lisboa, Portugal) for valuable critical reading of the manuscript.

References and Notes

(1) Bolard, J. *Biochim. Biophys. Acta* **1986**, *864*, 257.
(2) Mills, J.; Masur, H. *Sci. Am.* **1990**, *263*, 32.
(3) Stenberg, S. *Science* **1994**, *266*, 1632.
(4) de Kruijff, B.; Demel, R. A. *Biochim. Biophys. Acta* **1974**, *339*, 57.
(5) Miñones, J., Jr.; Miñones, J.; Conde, O.; Seoane, R.; Dynarowicz-Latka, P. *Langmuir* **2000**, *16*, 5743.
(6) Ockman, N. *Biochim. Biophys. Acta* **1974**, *345*, 263.
(7) Ockman, N. *Biochim. Biophys. Acta* **1974**, *373*, 481.
(8) Harrand, M.; Peticolas, W. L.; Dupeyrat, R. *Biochem. Biophys. Res. Commun.* **1982**, *104*, 1120.
(9) Dufourc, E. J.; Smith, I. C. P.; Jarrell, H. C. *Biochim. Biophys. Acta* **1984**, *776*, 317.
(10) Dufourc, E. J.; Smith, I. C. P. *Biochemistry* **1985**, *24*, 2420.
(11) Saint-Pierre-Chazalet, M.; Thomas, C.; Dupeyrat, M.; Gary-Bobo, C. M. *Biochim. Biophys. Acta* **1988**, *944*, 477.
(12) Seoane, R.; Miñones, J.; Conde, O.; Casas, M.; Iribarnegaray, E. *Biochim. Biophys. Acta* **1998**, *1375*, 73.

(13) Hing, A. W.; Scaefer, J.; Kabayashi, G. S. *Biochim. Biophys. Acta* **2000**, *1463*, 323.
(14) Miñones, J.; Carrera, C.; Dynarowicz-Latka, P.; Miñones, J.; Conde, O.; Seoane, R.; Patino, J. M. R. *Langmuir* **2001**, *17*, 1477.
(15) Castanho, M. A. R. B.; Santos, N. C.; Loura, L. M. S. *Eur. Biophys. J.* **1997**, *26*, 253.
(16) Bustamante, C.; Maestre, M. F. *Proc. Natl. Acad. Sci. U.S.A.* **1988**, *85*, 8482.
(17) Lopes, S.; Fernandes, M. X.; Prieto, M.; Castanho, M. A. R. B. *J. Phys. Chem. B* **2001**, *105*, 562.
(18) Kooyman, R. P. H.; Levine, Y. K.; Van der Meer, B. W. *Chem. Phys.* **1981**, *60*, 317.
(19) Coutinho, A.; Prieto, M. *Biophys. J.* **1995**, *69*, 2541.
(20) Coutinho, A. *Estudo do mecanismo de acção ao nível molecular do antibiótico poliénico nistatina por técnicas de fluorescência*, Ph.D. Thesis: Lisboa 2000, pp169 and 296.
(21) Lancelin, J.-M.; Paquet, F.; Beau, J.-M. *Tetrahedron Lett.* **1988**, *29*, 2827.
(22) Singer, M. A. *Can. J. Physiol. Pharmacol.* **1975**, *53*, 1072.
(23) Castanho, M. A. R. B.; Coutinho, A.; Prieto, M. *J. Biol. Chem* **1992**, *267*, 204.
(24) Fujii, G.; Chang, J.-F.; Coley, T.; Steer, B. *Biochemistry* **1997**, *36*, 4959.
(25) Nagle, J. F.; Tristram-Nagle, S. *Biochim. Biophys. Acta* **2000**, *1469*, 159.
(26) Shang, Q.; Hudson, B. S.; Dou, X. *Nature* **1991**, *352*, 703.
(27) Birge, R. R.; Zgierski, M. Z.; Serrano-Andres, L.; Hudson, B. S. *J. Phys. Chem. A* **1999**, *103*, 2251.
(28) Dolan, P. M.; Miller, D.; Cogdell, R. J.; Birge, R. R.; Frank, H. A. *J. Phys. Chem. B* **2001**, *105*, 12134.
(29) Haynes, M. P.; Chong, P. L.; Bucley, H. R.; Pieringer, R. A. *Biochemistry* **1996**, *35*, 7983.
(30) HsuChen, C.-C.; Feingold, D. S. *Biochem. Biophys. Res. Commun.* **1973**, *51*, 972.
(31) HsuChen, C.-C.; Feingold, D. S. *Antimicrob. Agents Chemother*. **1973**, *4*, 309.
(32) Archer, D. B. *Biochim. Biophys. Acta* **1976**, *436*, 68.
(33) Aracava, Y.; Schreier, S.; Phadke, R.; Deslauriers, R.; Smith, I. C. P. *Biophys. Chem.* **1981**, *14*, 325.
(34) Levin, I. W.; Lewis, E. N. *SPIE* **1989**, *1145*, 99.
(35) Roberts, G. G., Ed. *Langmuir*−*Blodgett films*; Plenum Press: New York, 1990.